Electronic Supplementary Material (ESI) for Lab on a Chip.

Supplementary Materials

TANDEM: Biomicrofluidic Systems with Transverse And Normal Diffusional Environments for Multidirectional Signalling

Michael D. Mohan and Edmond W. K. Young*

1 Experimental

1.1 Quantification of 10-kDa FITC-Dextran diffusion in two-channel geometry

Time lapse images for the 3-h period were converted to stacks in ImageJ and used to generate 8-bit values for average pixel intensity of ROIs located at the center of the left and right channels respectively. The original dataset (x), was then converted to a normalized dataset (z), by performing the following function on all elements within x:

$$z_i = \frac{x_i - \min(x)}{\max(x) - \min(x)}$$

The same operation was also performed on all simulated datasets produced by COMSOL. Left channel and right channel data for both measured and simulated species transport were then plotted from the normalized datasets and used in all further analyses.

2 Fundamental equations for computational modelling

Creeping flow in free-flow domains. In general, fluid flow within the control volume is governed by the Navier-Stokes equations for incompressible fluid motion:

$$\rho \frac{\partial \mathbf{u}}{\partial t} + \rho(\mathbf{u} \cdot \nabla)\mathbf{u} = \nabla \cdot [-p\mathbf{I} + \mathbf{T}] + \mathbf{F} \quad (1)$$

$$\nabla \cdot \mathbf{u} = 0 \quad (2)$$

$$\mathbf{T} = \mu[\nabla \mathbf{u} + (\nabla \mathbf{u})^T] \quad (3)$$

where ρ is the fluid density, μ represents the dynamic viscosity, $\mathbf{u}$ is the velocity field vector, p is pressure, $\mathbf{T}$ is the viscous stress tensor and $\mathbf{F}$ is the per-unit-volume body force vector. Given the characteristic velocity and length scale of the system, low Reynolds number laminar flow is valid ($Re \ll 1$), and the convective term above may be neglected. Additionally, in our case, body forces were considered negligible. This results in simplified Stokes flow within the channels:

$$\rho \frac{\partial \mathbf{u}}{\partial t} = \nabla \cdot [-p\mathbf{I} + \mu(\nabla \mathbf{u} + (\nabla \mathbf{u})^T)] \quad (4)$$

$$\nabla \cdot \mathbf{u} = 0 \quad (5)$$

Porous media flow. For transport within our hydrogel compartment, we used Darcy's Law of permeability to treat the hydrogel as a homogeneous porous medium (defined as a "matrix domain" in COMSOL):

$$\mathbf{u}_D = -\frac{\kappa}{\mu} \nabla p \quad (6)$$

$$\frac{\partial}{\partial t}(\rho \varepsilon) + \nabla \cdot (\rho \mathbf{u}_D) = Q_m \quad (7)$$

where $\mathbf{u}_D$ is the Darcy velocity field vector within the porous domain (often referred to as the superficial velocity), κ is the Darcy permeability of the porous medium, ε is the porosity, and Q_m is the mass source term. Equation (7) above is essentially the continuity equation as it pertains to porous media.

Mass transport of diluted species in free-flow domains. For a given nutrient species, *i*, a mass balance can be performed:

$$\frac{\partial c_i}{\partial t} + \nabla \cdot \mathbf{J}_i + \mathbf{u} \cdot \nabla c_i = R_i \ (8)$$

$$\mathbf{J}_i = -D_i \nabla c_i \ (9)$$

where $\mathbf{J}_i$ is the diffusive mass flux of species *i*, $\mathbf{u}$ is the mass-averaged velocity vector, c_i is the concentration of the species, D_i is the species diffusivity, and R_i is the reaction rate of the species. Note in this case that no reaction takes place, which results in the following system to define mass transport in the free-flow domains:

$$\frac{\partial c_i}{\partial t} + \nabla \cdot \mathbf{J}_i + \mathbf{u} \cdot \nabla c_i = 0 \ (10)$$

$$\mathbf{J}_i = -D_i \nabla c_i$$

Mass transport of diluted species in porous domains. While the previous set of equations is true for a free-flow (non-porous medium) domain, the equations require modification for a porous medium domain because diffusivity of a molecule in porous media must be lower than its diffusivity in free-flow. This creates a distinction between effective diffusivity and free-flow diffusivity of a species and real concentration gradient as compared to apparent concentration gradient. Millington and Quirk[1] have shown considerable accuracy in accounting for this by scaling the diffusivity using a ratio of the total porosity and tortuosity factor, τ of the porous medium:

$$\frac{\partial c_i}{\partial t} + \nabla \cdot \mathbf{J}_i + \mathbf{u} \cdot \nabla c_i = R_i + S_i \ (11)$$

$$\mathbf{J}_i = -D_{e,i} \nabla c_i \ (12)$$

$$D_{e,i} = \frac{\varepsilon}{\tau} D_{f,i} \ (13)$$

For porous solids with steady diffusive flow, Millington[2] also demonstrated that this tortuosity factor and total porosity can be related as shown:

$$\tau = \varepsilon^{-\frac{1}{3}} \quad (14)$$

resulting in the following:

$$D_{e,i} = \varepsilon^{\frac{4}{3}} D_{f,i} \quad (15)$$

In the above equations, S_i is an additional source/sink term for species i, $D_{e,i}$ is the effective diffusivity in porous media, and $D_{f,i}$ is the actual diffusivity of molecular species in an open fluid. Similarly, as above, Equation (11) reduces to Equation (10). The resulting set then describes mass transport of species *i,* in the porous media channel:

$$\frac{\partial c_i}{\partial t} + \nabla \cdot \mathbf{J}_i + \mathbf{u} \cdot \nabla c_i = 0$$

$$\mathbf{J}_i = -D_{e,i} \nabla c_i$$

$$D_{e,i} = \varepsilon^{\frac{4}{3}} D_{f,i}$$

Tissue barrier function of mass transport. Cell monolayers separating the side channels from the porous media in the middle channel can significantly affect lateral species transport. This highlights a key difference of these channels compared to the additional top channel (TC) of the DP design. The effects of diffusion due to the permeability of the monolayers can be modelled using a thin diffusion barrier separating the free-flow domain (subscript 1) and the porous domain (subscript 2):

$$-\mathbf{n} \cdot D_{s,i} \nabla c_{i,1} = \frac{D_{s,i}}{d_b}\left(c_{i,1} - c_{i,2}\right) \quad (16)$$

$$-\mathbf{n} \cdot D_{s,i} \nabla c_{i,2} = \frac{D_{s,i}}{d_b}\left(c_{i,2} - c_{i,1}\right) \quad (17)$$

In the equations above, d_b is the barrier thickness. Equations (16) and (17), along with the other equations highlighted in this section, provide a general governing set of equations for mass transport in our TANDEM microfluidic device.

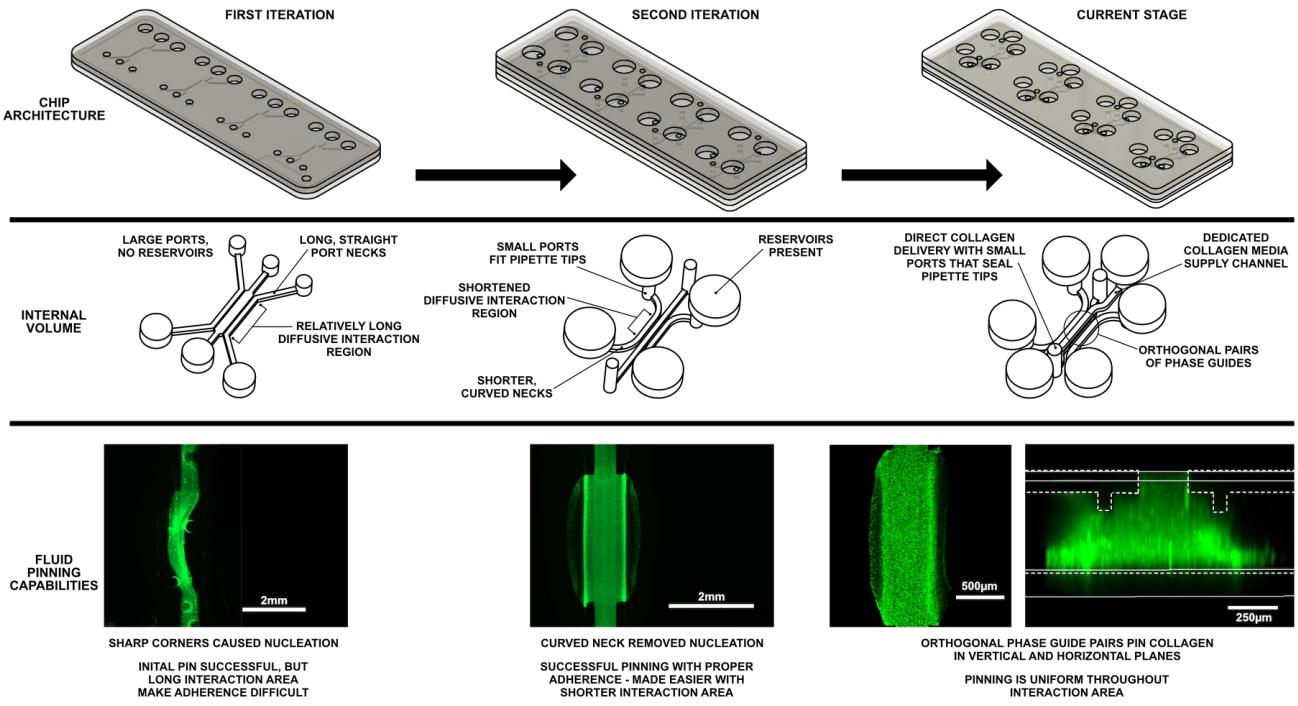

Figure S1: Design iteration progression. Three of the most notable iterations are shown. Initial designs involved relatively long port necks and phase guide lengths with sharp cornering and a lack of reservoirs. Intermediate designs improved gel pinning and reduced nucleation through the use of shortened phase guide lengths and curved geometries. Reservoirs were added to provide sufficient nutrient supply to cultures over a 24-h period. The current design builds upon these modifications by adding an upper channel system that is vertically accessible by the central channel to improve nutrient access to cells embedded in the gel. The lowest row of images shows the result of collagen polymerization within the device, visualized with green fluorescent micro beads.

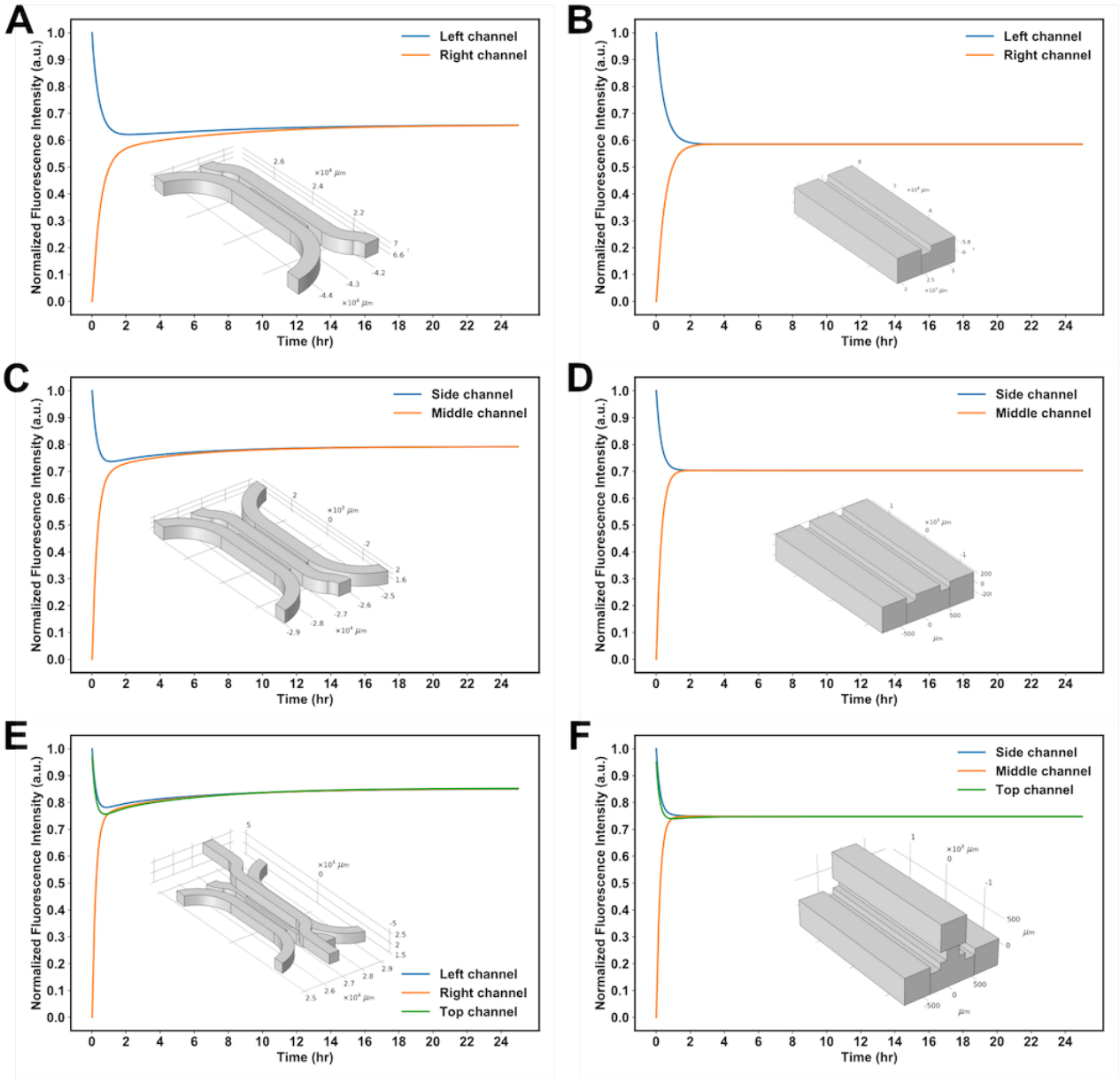

Figure S2: Significance of channel capacity in simulation models. (A) and (B) show the rates of species diffusion in a two-channel system over a 24-h time period for models including and omitting the channel geometries respectively. Similarly, (C), (D) and (E), (F) pairs show results for the three-channel (NTC) system and four-channel (TC) system respectively.

3 Supplementary References

1. Millington, R. J. & Quirk, J. P. Permeability of porous solids. *Trans. Faraday Soc.* **57**, 1200–1207 (1961).

2. Millington, R. J. Gas Diffusion in Porous Media. *Sci. (American Assoc. Adv. Sci.* **130**, 100–102 (1959).